Geophysical Research Letters

RESEARCH LETTER
10.1029/2019GL083149

Dissolved Organic Radiocarbon in the Central Pacific Ocean

Ellen R. M. Druffel[1], Sheila Griffin[1], Ning Wang[1,2], Noreen G. Garcia[1], Ann P. McNichol[3], Robert M. Key[4], and Brett D. Walker[1,5]

[1]Department of Earth System Science, University of California, Irvine, CA, USA, [2]State Key Laboratory of Isotope Geochemistry, Guangzhou Institute of Geochemistry, Chinese Academy of Sciences, Guangzhou, China, [3]National Ocean Sciences Accelerator Mass Spectrometry, Woods Hole Oceanographic Institution, Woods Hole, MA, USA, [4]Atmospheric and Oceanic Sciences Program, Princeton University, Princeton, NJ, USA, [5]Now at Department of Earth and Environmental Science, University of Ottawa, Ottawa, Ontario, Canada

Key Points:
- ^{14}C aging of dissolved organic and inorganic carbon in the bottom waters of the Pacific are equivalent
- Surface DOC $\Delta^{14}C$ values are low in equatorial and polar regions where upwelling occurs and high in the subtropics where downwelling dominates
- Minimum DOC $\Delta^{14}C$ values (-550 to -570 per mil) are observed in Pacific Deep Water north of the equator

Supporting Information:
- Supporting Information S1

Correspondence to:
E. R. M. Druffel,
edruffel@uci.edu

Citation:
Druffel, E. R. M., Griffin, S., Wang, N., Garcia, N. G., McNichol, A. P., Key, R. M., & Walker, B. D. (2019). Dissolved organic radiocarbon in the Central Pacific Ocean. *Geophysical Research Letters*, *46*, 5396–5403. https://doi.org/10.1029/2019GL083149

Received 3 APR 2019
Accepted 30 APR 2019
Accepted article online 2 MAY 2019
Published online 21 MAY 2019

Abstract We report marine dissolved organic carbon (DOC) concentrations, and DOC $\Delta^{14}C$ and $\delta^{13}C$ values in seawater collected from the central Pacific. Surface $\Delta^{14}C$ values are low in equatorial and polar regions where upwelling occurs and high in subtropical regions dominated by downwelling. A core feature of these data is that ^{14}C aging of DOC (682 ± 86 ^{14}C years) and dissolved inorganic carbon (643 ± 40 ^{14}C years) in Antarctic Bottom Water between 54.0°S and 53.5°N are similar. These estimates of aging are minimum values due to mixing with deep waters. We also observe minimum $\Delta^{14}C$ values (−550‰ to −570‰) between the depths of 2,000 and 3,500 m in the North Pacific, though the source of the low values cannot be determined at this time.

Plain Language Summary Most of the organic carbon in ocean water is in the dissolved form, like the broth in chicken soup. Even though it is believed that dissolved organic carbon (DOC) is formed during photosynthesis in the surface ocean using modern carbon, its radiocarbon age is surprisingly thousands of years old. We present the first transect of radiocarbon in DOC for the Pacific Ocean. We find that the radiocarbon age of DOC in the bottom waters decreases similarly to that found in the more abundant dissolved inorganic carbon. We conclude that DOC ages in the bottom water as it flows northward toward Alaska.

1. Introduction

Dissolved organic carbon (DOC) is the largest pool of organic carbon in the ocean, equal in size to carbon in the atmosphere (Hansell et al., 2009). The DOC in the deep North Pacific (>1,500 m) was found to be 6,000 ^{14}C years old in 1985 and 1987 (Druffel et al., 1992; Williams & Druffel, 1987). This very old age was surprising because DOC was thought to be produced in the surface ocean where ^{14}C levels are near modern ($\Delta^{14}C = -50‰$) and should be much younger. Instead, the old ^{14}C age indicates that, at least a portion of the DOC, survives multiple ocean mixing cycles. Our field has been intrigued by these results ever since.

It was proposed that the surface DOC is composed of a 1:1 mixture of old DOC, similar to the radiocarbon ($\Delta^{14}C$) value of deep water and newly produced, postbomb $\Delta^{14}C$ values (Williams & Druffel, 1987). There were few profiles of DOC $\Delta^{14}C$ in the open Pacific Ocean (Bauer et al., 1992; Bauer et al., 1998; Beaupré & Druffel, 2009; Druffel & Bauer, 2000) until recent studies contributed more data (Druffel et al., 2018; Druffel & Griffin, 2015; Griffith et al., 2012; Tanaka et al., 2010; Walker et al., 2016). The 1:1 mixture of old and postbomb $\Delta^{14}C$ values still holds in the recent data, but there are subtleties in the new profiles that had not been noticed previously. For example, the presence of bomb ^{14}C DOC was confirmed in parts of the deep North Atlantic, which lowered the prebomb $\Delta^{14}C$ estimate of deep DOC in this region from −390‰ to −456‰ (Druffel et al., 2016). In addition, DOC $\Delta^{14}C$ values in deep water from the central North Pacific decreased from the 1980s to 2015, indicating that there is spatial inhomogeneity and/or temporal variability of DOC isotopic compositions on decadal timescales (Druffel et al., 2018).

Here we show that deep DOC $\Delta^{14}C$ values from the central Pacific are consistent with transport of Antarctic Bottom Water (AABW) northward and that this aging is equivalent to that observed for DIC in this water mass.

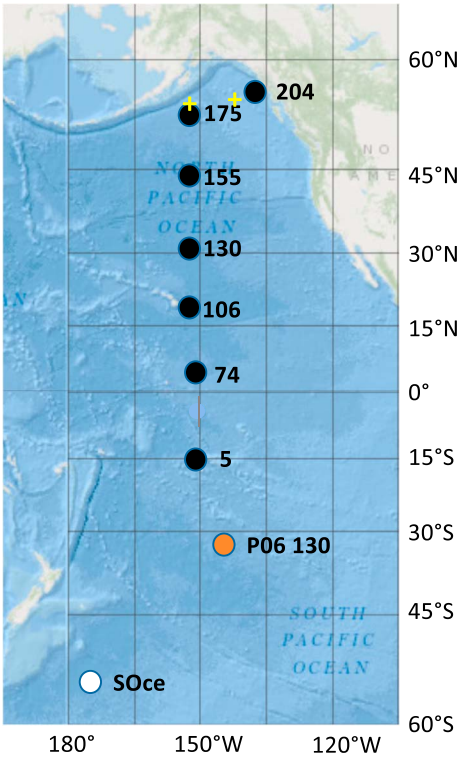

Figure 1. Map of the locations occupied on two legs of the P16N cruise in April–July 2015 (black circles) and the Gulf of Alaska cruise in 2013 (yellow crosses). Also shown are the locations for comparison data used in this paper: Southern Ocean cruise (white circle) in 1995 and P06 cruise (orange circle) in 2010.

2. Setting and Methods

Seawater DOC concentrations and isotopic values ($\Delta^{14}C$ and $\delta^{13}C$) were measured in samples collected from two cruises: (1) two legs of the GO-SHIP P16N cruise along 152°W from 14.5°S to 56.5°N aboard the NOAA vessel *Ronald H. Brown* (April–July 2015) and (2) in two deep samples from the Gulf of Alaska (GoA) collected in June 2013 aboard the *R/V Melville* (Figure 1). Data from one of these stations (130) were published by Druffel et al. (2018). DOC samples shallower than 400 m were filtered using precombusted (540 °C, 2 hr), GFF (0.7 μm) filters. All DOC samples were collected in precombusted, 1-L Amber Boston Round glass bottles with acid cleaned (10% HCl), Polytetrafluoroethylene (PTFE)-lined caps with additional PTFE sheet liners, and frozen at −20 °C until analysis.

In the lab, DOC samples were diluted with low carbon (DOC = 0.6 ± 0.3 μM), 18.2 Milli-Q water, acidified with 1-mL 85% phosphoric acid (HPLC grade), purged with ultrahigh purity helium gas, and ultraviolet oxidized for 4 hr in a quartz reactor (Beaupré et al., 2007; Griffin et al., 2010). The CO_2 evolved from DOC was stripped with ultrahigh purity helium gas, cryogenically purified, and quantified. Reported DOC concentrations were corrected for CO_2 loss due to breakthrough from the Horibe glass trap cooled with liquid nitrogen during collection, whose mass was quantified via integration using an infrared CO_2 gas analyzer (LI-COR Inc., model LI-6252; Walker et al., 2019). The breakthrough does not affect the $\Delta^{14}C$ and $\delta^{13}C$ measurements outside of the reported uncertainties. One sample replicate is run for every 14 samples (i.e., one per depth profile).

Samples were converted from CO_2 to graphite, by reduction on an iron catalyst using the closed-tube, zinc method (Walker & Xu, 2019; Xu et al., 2007). $\Delta^{14}C$ measurements were performed by us at the Keck Carbon Cycle AMS Laboratory at University of California, Irvine (Santos et al., 2010; Southon et al., 2004). Radiocarbon results are reported as $\Delta^{14}C$ values that are corrected for date of collection according to convention (Stuiver & Polach, 1977). Total uncertainty of the $\Delta^{14}C$ analyses are ±4‰ (Druffel et al., 2013; Walker et al., 2016).

The $\delta^{13}C$ value of each sample was measured on a split of the CO_2 that was produced from ultraviolet oxidation of the DOC sample using a Gas Bench II and Thermo Electron Delta Plus isotope ratio mass spectrometer, with a total analytical uncertainty of ±0.2‰.

3. Results

The DOC concentrations and $\delta^{13}C$ and $\Delta^{14}C$ measurements are plotted in latitudinal sections using Ocean Data View (Schlitzer, 2015; Figure 2), and depth profiles are presented in Figures S1–S3 in the supporting information. Data from two stations at 32.5°S and 54.0°S occupied on previous cruises are also shown in Figure 2.

3.1. DOC Concentrations

The DOC concentrations ([DOC]) were highest in the upper 100 m of the water column (58.1–83.9 μM; Table S2 and Figure S1 in the supporting information and Figure 2a). Concentrations decreased rapidly by 900 m across the Pacific and ranged from 35.8–43.4 μM below 1,000 m. The average [DOC] values below 1,000 m for most stations were within error, ranging from 38.4 ± 1.5 μM (stn 106) to 40.2 ± 1.9 μM (stn 155). The average at the slope station off Alaska was the highest (41.7 ± 0.6 μM; stn 204). These values are within statistical uncertainty to averages of [DOC] measurements reported for nearby stations on this P16N cruise (Carlson, 2018).

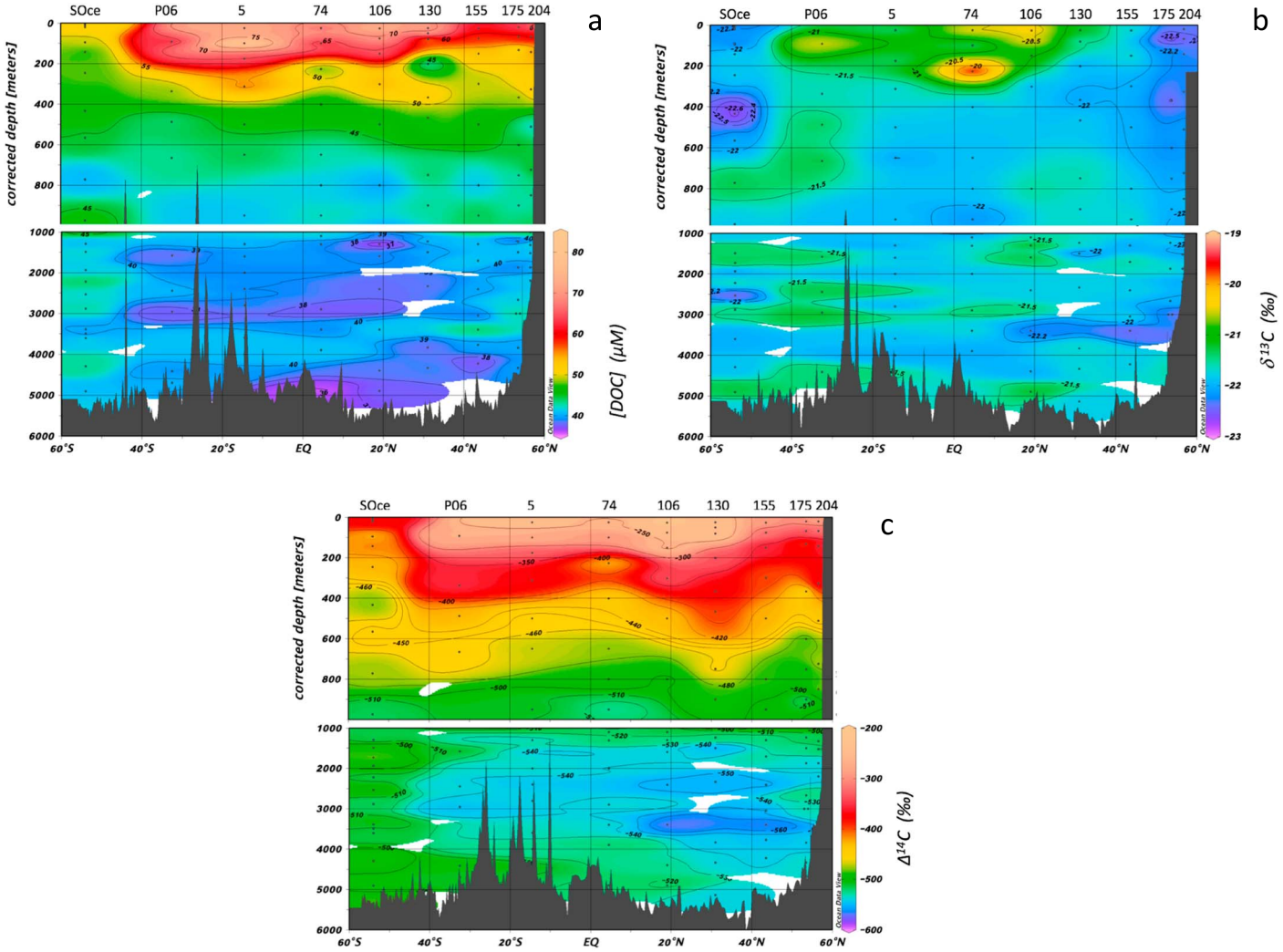

Figure 2. (a) Dissolved organic carbon (DOC) concentrations (μM), (b) DOC $\delta^{13}C$ values (‰), and (c) DOC $\Delta^{14}C$ values (‰) of water samples collected from seven stations on two legs of the P16N cruise in 2015 (this work), one station on the P06 cruise (stn 130, 32.5°S 144.7°W) in 2010 (Druffel & Griffin, 2015) and one station from the Southern Ocean (SOce; 54.0°S 176.0°W) in 1995 (Druffel & Bauer, 2000) using Ocean Data View (Schlitzer, 2015).

3.2. DOC $\delta^{13}C$ Values

The DOC $\delta^{13}C$ values ranged from −22.7‰ to −20.3‰ in the upper 950 m (Table S2 and Figure S2 in the supporting information and Figure 2b). Values were less variable below 1,000 m, ranging from −22.1 to −21.2‰, with the exception of three low values between 3,000 and 3,400 m (−22.6 to −22.3‰) at stations 106, 155, and GoA 10. Overall, the average $\delta^{13}C$ value for each station below 1,000 m ranged from −22.0 ± 0.1‰ (stns 5 and 204) to −21.6 ± 0.4‰ (stn 106).

3.3. DOC $\Delta^{14}C$ values

The DOC $\Delta^{14}C$ values for samples collected from seven stations on the P16N cruise ranged from −294‰ to −213‰ in the surface ocean (20–26 m; Figure 2c and Table S2 in the supporting information). Lower values (−294‰ to −258‰) were observed for samples at high latitudes and near the equator (stns 74, 155, 175, and 204). Values decreased quickly in the upper 1,000 m, which include Subantarctic Mode Water (SAMW), Antarctic Intermediate Water (AAIW), and North Pacific Intermediate Water (NPIW; see section 4.1). The DOC $\Delta^{14}C$ values below 1,000 m ranged from −570‰ to −513‰ (both at stn 106). The lowest values were found in the Pacific Deep Water (PDW) between 2,000 and 3,500 m (sigma3 41.32–41.47) and ranged from an average of −538 ± 3‰ at 4.5°N (stn 74) to −560 ± 14‰ at 19°N (stn 106). The two deep samples from the GoA cruise (3,000

and 3,005 m) averaged −532 ± 2‰. Below 2,000 m, the DOC $\Delta^{14}C$ values at the southern stations (5, 74, and 106) were generally higher by 10–20‰ than those at the northern stations (130, 155, 175, and 204; Figure 2c).

4. Discussion

The discussion is presented in five parts. First, we discuss the presence of bomb ^{14}C in DOC of the upper 1,000 m of the Pacific water column, which includes both the SAMW and intermediate water masses. Second, we present a comparison of the $\Delta^{14}C$ values of DOC and dissolved inorganic carbon (DIC) throughout the water column. Third, we discuss the ^{14}C aging of DOC and DIC in the AABW of the Pacific. Here implications are discussed regarding the primary control on DOC ^{14}C aging in the deep Pacific Ocean. Fourth, we discuss the unusually low DOC $\Delta^{14}C$ and $\delta^{13}C$ values at ~3,400-m depth in the North Pacific and possible explanations for these low isotopic values. Fifth, we place these results into the context of recent work that revealed temporal variability in deep DOC $\Delta^{14}C$ values (Druffel et al., 2018).

Along with our DOC $\Delta^{14}C$ measurements from the central Pacific (P16N and GoA), we include previously published DOC $\Delta^{14}C$ profiles from the SOce (at 54.0°S 176.0°W) in 1995 (Druffel & Bauer, 2000) and the South Pacific (P06 at 32.5°S 144.6°W) in 2010 (Druffel & Griffin, 2015) for comparison. The SOce samples were collected in 1995, 20 years before the P16N cruise; however, the average of DOC $\Delta^{14}C$ values (−490 ± 10‰ $n = 6$) from samples deeper than 1,500 m collected at the same latitude, but south of the Indian Ocean in 2016 (Bercovici et al., 2018), are within uncertainty of the average of those from the SOce cruise (−500 ± 12‰ $n = 14$). Also of note, the uncertainty of $\delta^{13}C$ values for the P06 station (±0.5‰) are higher than those for the P16N and GoA cruises (±0.2‰).

4.1. DOC Isotopic Distributions in Water Masses of the Upper Ocean

DOC $\Delta^{14}C$ values in the upper 900 m of the water column are higher than −522‰ (Table S2 in the supporting information) and may contain bomb ^{14}C. This is similar to DIC $\Delta^{14}C$ results in the central Pacific (<1,000 m) during the 1970s (Ostlund & Stuiver, 1980) and the 1990s (Key et al., 2004) that were shown to contain bomb ^{14}C. The highest DOC $\Delta^{14}C$ values (>−250‰) are found in the surface of the subtropical Pacific (stns 5, 106, and 130), where downwelling is dominant. Lower surface values are found at higher latitudes (−294‰ to −276‰), and to a lesser extent, near the equator (−258‰), where deeper isopycnals intersect the sea surface, bringing lower $\Delta^{14}C$ waters to the surface. This upwelling is especially intense in the SOce where surface DOC $\Delta^{14}C$ values lower than −400‰ are found (Bercovici et al., 2018; Druffel & Bauer, 2000).

Another surface feature is the correlation between DOC $\delta^{13}C$ values (from 20- to 26-m depth) and sea surface temperatures (SSTs; Figure S4a in the supporting information). Rau et al. (1989) reported that the correlation between plankton $\delta^{13}C$ values and SST was actually attributed to a first-order, inverse relationship between plankton $\delta^{13}C$ and dissolved CO_2 concentration [$CO_{2\ aq}$], presumably due to intracellular carbon fixation. To our knowledge, these are the first data that show a correlation between surface DOC $\delta^{13}C$ and SST. There was no significant correlation between our DOC $\delta^{13}C$ values and [$CO_{2\ aq}$] (Figure S4b in the supporting information; Wanninkhof, 2019a, 2019b; Dickson, 2019a, 2019b; Millero, 2015). This relationship is consistent with surface primary producers imparting their carbon isotopic signature, as the main source of DOC in the surface ocean.

Produced in the subantarctic region of the southwest Pacific is SAMW (sigma0 25.4–26.9, ~200–500 m), which flows north toward the equator and eastward in the Equatorial Undercurrent (Rodgers et al., 2003; Toggweiler et al., 1991). Our samples in SAMW lie between 32.5°S (P06 stn 130) and 4.5°N (stn 74), and have DOC $\Delta^{14}C$ values ranging from −460‰ to −350‰ (Figure 2c and Table S2 in the supporting information). AAIW is formed in the Antarctic convergence zone (50°–60°S) and has moderately low salinity (34.3–34.5) and density (sigma0 26.82–27.43). Our samples in AAIW extend from 54.0°S (SOce) to 4.5°N (stn 74) and have DOC $\Delta^{14}C$ values ranging from −530‰ to −410‰ (Figure 2c and Table S2 in the supporting information). In both water masses, there is no discernable trend in DOC $\Delta^{14}C$ with latitude, suggesting that the water masses are too young for demonstrable DOC ^{14}C aging to be observed.

NPIW is produced in the northwestern subtropical gyre and has a minimum salinity (33.9–34.1, Talley, 1993; density sigma0 26.6–26.9). Our samples from the NPIW are from ~300- to 750-m depth between 19.5°N (stn

106) and 43.5°N (stn 155) and have DOC $\Delta^{14}C$ values ranging from −455‰ to −395‰ (Figure 2c and Table S2 in the supporting information).

4.2. Comparison Between $\Delta^{14}C$ of DOC and DIC in the Pacific

There is a significant correlation ($r^2 = 0.903$) between DOC $\Delta^{14}C$ (this work) and DIC $\Delta^{14}C$ (McNichol & Key, 2019a, 2019b) values obtained from water from the same Niskin bottles at the seven stations of the P16N cruise (Figure S5 in the supporting information). This correlation indicates that DOC and DIC $\Delta^{14}C$ values are coupled throughout the water column, as was shown previously using data from four locations in the Atlantic, Pacific, and Southern Oceans (Beaupré & Aluwihare, 2010). The presence of bomb ^{14}C was reported in DIC down to ~1,000-m depth in the Pacific Ocean (Key et al., 2004), using the method to separate the natural and bomb-produced ^{14}C based on the strong correlation between natural ^{14}C and potential alkalinity (Rubin & Key, 2002). Given the significant correlation between DOC and DIC $\Delta^{14}C$ values in 2015, it would follow that bomb ^{14}C is also present in DOC no deeper than 1,000-m depth as well in 2015. If this is the case, then it appears that dissolution and/or enzymatic hydrolysis of surface-derived particles over the past several decades has not been sufficient to change the average DOC $\Delta^{14}C$ value significantly (>2 sigma or 8‰) in the deep Pacific. DOC $\Delta^{14}C$ measurements in the deep North Pacific (31°N) decreased between the 1980s and 2015, the opposite of what one would expect had bomb ^{14}C been admitted to the deep sea (Druffel et al., 2018; see section 4.5).

4.3. ^{14}C Aging of DOC in AABW From the Southern Ocean to the Central North Pacific

The deepest part of the global overturning circulation is AABW, which is formed in the Southern Ocean and flows northward (below ~4,000-m depth, sigma4 > 45.85; Lavergne et al., 2017; Roussenov, 2004). In order to understand the primary control on DOC cycling in the deep Pacific, we present ^{14}C ages for DOC in samples with sigma4 > 45.85 versus latitude (Figure 3a). A significant linear trend is apparent using a Model II geometric mean regression of all points ($r^2 = 0.80$). Using this relationship, the difference between the DOC ^{14}C age at 54.0°S (5,619 ± 43 years) and 53.5°N (6,301 ± 43) is 682 ± 86 ^{14}C years. We also plot the DIC ^{14}C ages for samples with sigma4 > 45.85 (Druffel & Bauer, 2000; McNichol & Key, 2015; McNichol & Key, 2019a, 2019b) versus latitude from the same cruises as those portrayed in Figure 3b. The Model II geometric mean regression also displays a significant relationship (Figure 3b, $r^2 = 0.87$). The difference between the DIC ^{14}C age at 54.0°S (1,485 ± 20 years) and 53.5°N (2,128 ± 20 years) is 643 ± 40 ^{14}C years. This difference is equivalent to that obtained for DOC. In addition, the Model II regression slopes for both DOC (6.34 ± 0.80) and DIC (5.98 ± 0.38) versus latitude are within statistical uncertainty.

This aging is a minimum estimate, because of mixing that the bottom water experiences with the water above (Lavergne et al., 2017; Roussenov, 2004). This mixing-driven buoyancy flux causes the density of AABW to decrease as it travels northward in the Pacific (Lavergne et al., 2017). Mixing is "forced" to happen as the various isopycnals run into the bottom and is compounded by the fact that the Pacific shoals as one moves northward. Thus, we conclude that both DOC and DIC undergo similar ^{14}C aging as AABW travels northward. This interpretation is consistent with the aging of DIC in the deep Pacific estimated to represent the transit time of deep water in the major oceans (Stuiver et al., 1983).

4.4. Low DOC $\Delta^{14}C$ and $\delta^{13}C$ Values in PDW

Because there is no dense water formed in the North Pacific, the only source of water to the PDW is from upwelled AABW (Talley, 2013). PDW flows southward from the North Pacific between ~3,500 and 2,000 m (sigma3 41.25–41.47). There is a minimum in DOC $\Delta^{14}C$ values in PDW in the North Pacific that ranges from −550‰ to −570‰. DOC $\Delta^{14}C$ values in PDW increase with latitude south (Figure 2c). There is also a minimum in DIC $\Delta^{14}C$ values in PDW in the North Pacific that ranges from −250‰ to −210‰ (McNichol & Key, 2019a, 2019b; Figure S6 in the supporting information). Like DOC $\Delta^{14}C$ values, the DIC $\Delta^{14}C$ values increase with latitude south. The reverse aging is likely due to mixing of water from above and below the PDW, which acts to increase the $\Delta^{14}C$ values of the DOC and DIC in the PDW water mass as it travels southward.

Additionally, there are minima in DOC $\delta^{13}C$ values (<−21.9‰) at three stations (106, 155, and GoA 10) at ~3,400 m in the North Pacific (Figure S2 in the supporting information). Two of these low $\delta^{13}C$ values (−22.3‰ at stn 106 and −22.4‰ at stn 155) coincide with minimum DOC $\Delta^{14}C$ values (−570‰ and

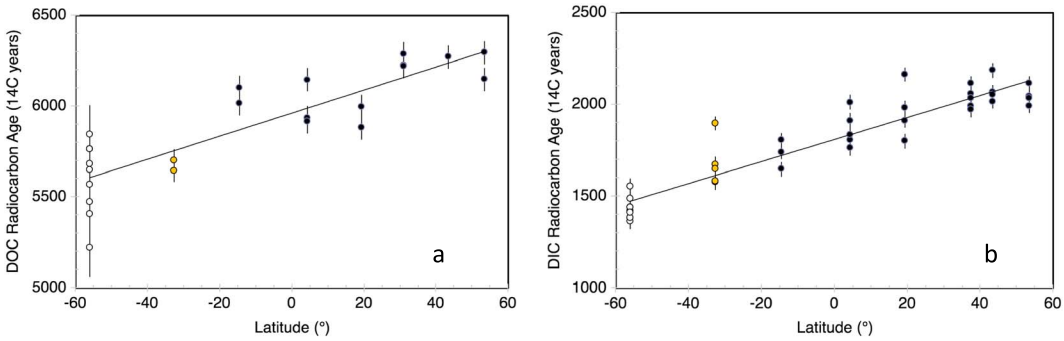

Figure 3. (a) Dissolved organic carbon (DOC) ^{14}C age versus latitude and (b) dissolved inorganic carbon (DIC) ^{14}C age versus latitude for samples with sigma4 > 45.85 (Antarctic Bottom Water). Data are from the P16N cruise in the central Pacific (this work; McNichol & Key, 2019a, 2019b; black circles), SOce (in 1995, white circles; Druffel & Bauer, 2000), and the South Pacific (P06 stn 130 in 2010; Druffel & Griffin, 2015; McNichol & Key, 2015; orange circles). The lines are Model II geometric mean regressions of all points. The equation for (a) is $6.34 \cdot x + 5{,}961.5$ (slope of 6.34 ± 0.80 and y intercept of $5{,}961.5 \pm 33.6$, $r^2 = 0.80$). The equation for (b) is $y = 5.98 \cdot x + 1{,}808.3$ (slope of 5.98 ± 0.38 and y intercept of $1{,}808.3 \pm 15.1$, $r^2 = 0.87$).

−565‰, respectively; Figure S3b in the supporting information). In addition, the [DOC] values for these two samples (41.2 ± 1.0 μM at stn 106 and 43.4 ± 1.0 μM at stn 155) are significantly higher than the averages of values (excluding the 3,400-m values) below 1,000 m (37.9 ± 1.5 and 39.6 ± 1.3 μM, respectively; Figure S1 in the supporting information).

The low isotopic values at ~3,400 m were not caused by preferential utilization of young DOC, because the [DOC] values were higher in these samples. There could have been recycling of bulk DOC via heterotrophy in these oldest DOC waters, contributing to the 1‰ shift in $\delta^{13}C$ values. However, if DOC was being consumed and produced with the bulk $\Delta^{14}C$ signature, there would have been no change in DOC $\Delta^{14}C$ or [DOC] values. It is possible, though unlikely, that the low $\delta^{13}C$ and $\Delta^{14}C$ values at ~3,400-m depth in the North Pacific could have come from a source of old, ^{13}C depleted carbon, for example, off-axis, hydrothermal systems that contain chemoautotrophically produced DOC (Lang et al., 2006) with low $\Delta^{14}C$ and low $\delta^{13}C$ (McCarthy et al., 2011). However, there are no active vent sites or ridges along this transect north of the equator, making this explanation unlikely. More data are needed to attribute the anomalously low DOC $\Delta^{14}C$ and $\delta^{13}C$ values to any one source or process.

4.5. Temporal and Spatial Variability in Deep DOC $\Delta^{14}C$

Temporal variability of DOC $\Delta^{14}C$ values was observed in the deep central North Pacific, where reoccupation of the same area in 1985, 1987, and 2015 revealed average DOC $\Delta^{14}C$ values (from depths >1,500 m) of −530 ± 6‰, −522 ± 5‰, and −544 ± 5‰, respectively (Druffel et al., 2018). Additionally, seasonal studies of a timeseries site in the northeast Pacific (Station M, 34.83°N 123.00°W) from 1991–2004 revealed variability throughout the water column in DOC $\Delta^{14}C$ values (20–60‰; Bauer et al., 1998; Beaupré & Druffel, 2009) that exceeded methodological uncertainty (±4–6‰). The results from Station M and the central North Pacific are consistent in indicating that temporal and spatial variability is present in the DOC $\Delta^{14}C$ signature in the deep Pacific. Therefore, it is likely that the DOC $\Delta^{14}C$ data we report here are also subject to variability. Notwithstanding, the presence of a significant gradient (682 ± 86 ^{14}C years) in the DOC ^{14}C ages with latitude in AABW that match that in the DIC (643 ± 40 ^{14}C years) suggests that the temporal and/or spatial variability is smaller than the aging of DOC in the waters transported northward in this water mass.

5. Implications for the Marine DOC Cycle

We show that the main trend of ^{14}C aging in AABW is similar for DOC and DIC, suggesting that the main control on the transport of both forms of carbon in the deep Pacific is decay during northward transport. As the oceans warm, changes in deep ocean circulation are likely to take place and perhaps cause changes in the residence time of organic matter in the deep sea. Moore et al. (2018) reported that by the year 2300, intense nutrient trapping in the Southern Ocean will cause redistribution of nutrients to the deep ocean, leaving the upper ocean depleted in nutrients and fisheries decreased. The questions of how the marine DOC cycle has changed in the past and may change in the future is open.

Letscher et al. (2016) confirm the importance of lateral transport of nutrients across the subtropical gyre margins for maintaining the level of observed ocean productivity. If DOC is also transported across gyre margins, and if upper ocean circulation changes centennially, then the DOC concentration and/or $\Delta^{14}C$ signature may change as well. Shen and Benner (2018) report that the size of the refractory DOC pool in the ocean could increase as circulation slows. Assessment of the variability of the residence time of DOC in the surface and deep ocean would be important for understanding how the global carbon cycle will change as the Earth's climate shifts.

Acknowledgments
We thank Jennifer Walker, Xiaomei Xu, and Dachun Zhang for their help with the stable carbon isotope measurements; John Southon and staff of the Keck Carbon Cycle AMS Laboratory for their assistance and advice; the support of chief scientists Samantha Siedlecki, Molly Baringer, Alison Macdonald, and Sabine Mecking; the guidance of Jim Swift and Dennis Hansell for shared ship time; and Sarah Bercovici for collecting water on the GoA cruise. We appreciate the comments of Christian Lewis and Niels Hauksson on this manuscript. This work was supported by NSF (OCE-141458941 to E. R. M. D. and OCE-0824864, OCE-1558654, and Cooperative Agreement OCE1239667 to R. M. K. and A. P. M.), the Fred Kavli Foundation, the Keck Carbon Cycle AMS Laboratory, and the NSF/NOAA-funded GO-SHIP Program. This research was undertaken, in part, thanks to funding from the Canada Research Chairs program (to B. D. W.) and an American Chemical Society Petroleum Research Fund New Directions grant (55430-ND2 to E. R. M. D. and B. D. W.). Data from the P16N cruises are available in Table S2 in the Supporting Information and at the Repeat Hydrography Data Center at the CCHDO website (http://cdiac.esd.ornl.gov/oceans/index.html) using the expo codes 3RO20150329, 3RO20150410, and 3RO20150525. There are no real or perceived financial conflicts of interests for any author.

References

Bauer, J. E., Druffel, E. R. M., Williams, P. M., Wolgast, D. M., & Griffin, S. (1998). Inter- and intra-annual variability in isotopic (^{14}C and ^{13}C) signatures of dissolved organic carbon in the eastern North Pacific Ocean. *Journal of Geophysical Research*, *103*(C2), 2867–2881. https://doi.org/10.1029/97JC02545

Bauer, J. E., Williams, P. M., & Druffel, E. R. M. (1992). ^{14}C activity of dissolved organic carbon fractions in the north central Pacific and Sargasso Sea. *Nature*, *357*(6380), 667–670. https://doi.org/10.1038/357667a0

Beaupré, S. R., & Aluwihare, L. (2010). Constraining the 2-component model of marine dissolved organic radiocarbon. *Deep Sea Research Part II: Topical Studies in Oceanography*, *57*(16), 1494–1503. https://doi.org/10.1016/j.dsr2.2010.02.017

Beaupré, S. R., & Druffel, E. R. M. (2009). Constraining the propagation of bomb-radiocarbon through the dissolved organic carbon (DOC) pool in the northeast Pacific Ocean. *Deep Sea Research Part I: Oceanographic Research Papers*, *56*(10), 1717–1726. https://doi.org/10.1016/j.dsr.2009.05.008

Beaupré, S. R., Druffel, E. R. M., & Griffin, S. (2007). A low-blank photochemical extraction system for concentration and isotopic analyses of marine dissolved organic carbon. *Limnology and Oceanography Methods*, *5*(6), 174–184. https://doi.org/10.4319/lom.2007.5.174

Bercovici, S. K., McNichol, A. P., Xu, L., & Hansell, D. A. (2018). Radiocarbon content of dissolved organic carbon in the South Indian Ocean. *Geophysical Research Letters*, *45*(2), 872–879. https://doi.org/10.1002/2017GL076295

Carlson, C. (2018). DOC/DON data from P16N cruise in 2015. expo code 33RO20150419. https://doi.org/10.7942/C2WC7C

Dickson, A. G. (2019a). Total alkalinity data from P16N cruise leg 1 in 2015. expo code 33RO20150419. https://doi.org/10.7942/C2WC7C

Dickson, A. G. (2019b). Total alkalinity data from P16N cruise leg 2 in 2015. expo code 33RO20150525. https://doi.org/10.7942/C2RP43

Druffel, E. R. M., & Bauer, J. E. (2000). Radiocarbon distributions in Southern Ocean dissolved and particulate organic carbon. *Geophysical Research Letters*, *27*(10), 1495–1498. https://doi.org/10.1029/1999GL002398

Druffel, E. R. M., & Griffin, S. (2015). Radiocarbon in dissolved organic carbon of the South Pacific Ocean. *Geophysical Research Letters*, *42*, 4096–4101. https://doi.org/10.1002/2015GL063764

Druffel, E. R. M., Griffin, S., Walker, B. D., & Coppola, A. I. (2016). Radiocarbon in dissolved organic carbon of the Atlantic Ocean. *Geophysical Research Letters*, *43*, 5279–5286. https://doi.org/10.1002/2016GL068746

Druffel, E. R. M., Griffin, S., Walker, B. D., Coppola, A. I., & Glynn, D. S. (2013). Total uncertainty of radiocarbon measurements of marine dissolved organic carbon and methodological recommendations. *Radiocarbon*, *55*(3), 1135–1141. https://doi.org/10.1017/S0033822200048049

Druffel, E. R. M., Griffin, S., Wang, N., & Walker, B. D. (2018). Temporal variability of dissolved organic radiocarbon in the deep North Pacific Ocean. *Radiocarbon*, *60*(4), 1115–1123. https://doi.org/10.1017/RDC.2018.39

Druffel, E. R. M., Williams, P. M., Bauer, J. E., & Ertel, J. (1992). Cycling of dissolved and particulate organic matter in the open ocean. *Journal of Geophysical Research*, *97*(C10), 15639–15659. https://doi.org/10.1029/92JC01511

Griffin, S., Beaupré, S. R., & Druffel, E. R. M. (2010). An alternate method of diluting dissolved organic carbon seawater samples for ^{14}C analysis. *Radiocarbon*, *52*(3), 1224–1229. https://doi.org/10.1017/S0033822200046300

Griffith, D. R., McNichol, A. P., Xu, L., McLaughlin, F. A., McDonald, R. W., Brown, K. A., & Eglinton, T. I. (2012). Carbon dynamics in the western Arctic Ocean: Insights from full-depth carbon isotope profiles of DIC, DOC, and POC. *Biogeosciences*, *9*(3), 1217–1224. https://doi.org/10.5194/bg-9-1217-2012

Hansell, D. A., Carlson, C. A., Repeta, D., & Schlitzer, R. (2009). Dissolved organic matter in the ocean: New insights stimulated by a controversy. *Oceanography Magazine*, *22*(4), 202–211. https://doi.org/10.5670/oceanog.2009.109

Key, R. M., Kozyr, A., Sabine, C. L., Lee, K., Wanninkhof, R., Bullister, J. L., et al. (2004). A global ocean carbon climatology: Results from Global Data Analysis Project (GLODAP). *Global Biogeochemical Cycles*, *18*, GB4031. https://doi.org/10.1029/2004GB002247

Lang, S. Q., Butterfield, D. A., Lilley, M. D., Johnson, H. P., & Hedges, J. I. (2006). Dissolved organic carbon in ridge-axis and ridge-flank hydrothermal systems. *Geochimica et Cosmochimica Acta*, *70*(15), 3830–3842. https://doi.org/10.1016/j.gca.2006.04.031

Lavergne, C. d., Madec, G., Roquet, F., Holmes, R. M., & McDougall, T. J. (2017). Abyssal ocean overturning shaped by seafloor distribution. *Nature*, *551*(7679), 181–186. https://doi.org/10.1038/nature24472

Letscher, R. T., Primeau, F., & Moore, J. K. (2016). Nutrient budgets in the subtropical ocean gyres dominated by lateral transport. *Nature Geoscience*, *9*(11), 815–819. https://doi.org/10.1038/NGEO2812

McCarthy, M. D., Beaupré, S. R., Walker, B. D., Voparil, I., Guilderson, T. P., & Druffel, E. R. M. (2011). Chemosynthetic origin of 14C-depleted dissolved organic matter in a ridge-flank hydrothermal system. *Nature Geoscience*, *4*(1), 32–36. https://doi.org/10.1038/ngeo1015

McNichol, A. P., & Key, R. (2015). DIC-14C data from P06E cruise in 2010. expo code 318M20100105. https://cchdo.ucsd.edu/cruise/318M20100105

McNichol, A. P., & Key, R. (2019a). DIC-14C data from P16N cruise leg 1 in 2015. expo code 33RO20150419. https://doi.org/10.7942/C2WC7C

McNichol, A. P., & Key, R. (2019b). DIC-14C data from P16N cruise leg 2 in 2015. expo code 33RO20150525. https://doi.org/10.7942/C2RP43

Millero, F. (2015). CO2 and total alkalinity data from P06E cruise in 2010. expo code 318M20100105. https://cchdo.ucsd.edu/cruise/318M20100105

Moore, J. K., Weiwei, F., Primeau, F., Britten, G. L., Lindsay, K., Long, M., et al. (2018). Sustained climate warming drives declining marine biological productivity. *Science*, *359*(6380), 1139–1143. https://doi.org/10.1126/science.aao6379

Ostlund, H. G., & Stuiver, M. (1980). Geosecs Pacific radiocarbon. *Radiocarbon*, *22*(01), 25–53. https://doi.org/10.1017/S0033822200004707

Rau, G. H., Takahashi, T., & Des Marias, D. J. (1989). Latitudial variations in plankton $\delta^{13}C$: Implications for CO_2 and productivity in past oceans. *Nature*, *341*(6242), 516–518. https://doi.org/10.1038/341516a0

Rodgers, K. B., Blanke, B., Madec, G., Aumont, O., Ciais, P., & Dutay, J.-C. (2003). Extratropical sources of equatorial Pacific upwelling in an OGCM. *Geophysical Research Letters*, *30*(2), 1084. https://doi.org/10.1029/2002GL016003

Roussenov, V. (2004). Role of bottom water transport and diapycnic mixing in determining the radiocarbon distribution in the Pacific. *Journal of Geophysical Research*, *109*, C06015. https://doi.org/10.1029/2003JC002188

Rubin, S. I., & Key, R. M. (2002). Separating natural and bomb-produced radiocarbon in the ocean: The potential alkalinity method. *Global Biogeochemical Cycles*, *16*(4), 1105. https://doi.org/10.1029/2001GB001432

Santos, G. M. J. R., Southon, N. J. D., Ziolkowski, L., Druffel, E. R. M., Xu, X., Zhang, D., et al. (2010). Blank assessment for ultra–small radiocarbon samples: Chemical extraction and separation vs AMS. *Radiocarbon*, *52*(3), 1322–1335. https://doi.org/10.1017/S0033822200046415

Schlitzer, R. (2015). Ocean data view. http://odv.awi.de

Shen, Y., & Benner, R. (2018). Mixing it up in the ocean carbon cycle and the removal of refractory dissolved organic carbon. *Scientific Reports*, *8*(1). https://doi.org/10.1038/s41598-018-20857-5

Southon, J. R., Santos, G. M., Druffel-Rodriguez, K. C., Druffel, E. R. M., Trumbore, S. E., Xu, X., et al. (2004). The Keck Carbon Cycle AMS Laboratory, U.C.I.: Initial operation and a background surprise. *Radiocarbon*, *46*(01), 41–49. https://doi.org/10.1017/S0033822200039333

Stuiver, M., & Polach, H. A. (1977). Discussion: Reporting of ^{14}C data. *Radiocarbon*, *19*(03), 355–363. https://doi.org/10.1017/S0033822200003672

Stuiver, M., Quay, P. D., & Ostlund, H. G. (1983). Abyssal water 14C distribution and the age of the world oceans. *Science*, *219*(4586), 849–851. https://doi.org/10.1126/science.219.4586.849

Talley, L. D. (1993). Distribution and formation of North Pacific intermediate water. *Journal of Physical Oceanography*, *23*(3), 517–537. https://doi.org/10.1175/1520-0485(1993)023<0517:DAFONP>2.0.CO;2

Talley, L. D. (2013). Closure of the global overturning circulation through the Indian, Pacific, and Southern Oceans: Schematics and transports. *Oceanography Magazine*, *26*(1), 80–97. https://doi.org/10.5670/oceanog.2013.07

Tanaka, N., Otosaka, S., Wakita, M., Amano, H., & Togawa, O. (2010). Preliminary result of dissolved organic radiocarbon in the western North Pacific Ocean. *Nuclear Instruments and Methods Physics Research*, *268*(7-8), 1219–1221. https://doi.org/10.1016/j.nimb.2009.10.137

Toggweiler, J. R., Dixon, K., & Broecker, W. S. (1991). The Peru upwelling and the ventilation of the South Pacific thermocline. *Journal of Geophysical Research*, *96*(C11), 20,467–20,497. https://doi.org/10.1029/91JC02063

Walker, B. D., Beaupré, S. R., Griffin, S., & Druffel, E. R. M. (2019). UV photochemical oxidation and extraction of marine dissolved organic carbon at UC Irvine: Status, surprises, and methodological recommendations. *Radiocarbon*, 1–15. https://doi.org/10.1017/RDC.2019.9

Walker, B. D., Griffin, S., & Druffel, E. R. M. (2016). Effect of acidified versus frozen storage on marine dissolved organic carbon concentration and isotopic composition. *Radiocarbon*, *59*(3), 843–857. https://doi.org/10.1017/RDC.2016.48

Walker, B. D., & Xu, X. (2019). An improved method for the sealed-tube zinc graphitization of microgram carbon samples and ^{14}C AMS measurement. *Nuclear Instruments & Methods in Physics Research Section B-Beam Interactions with Materials and Atoms*, *438*, 58–65. https://doi.org/10.1016/j.nimb.2018.08.004

Wanninkhof, R. (2019a). TCO2 data from P16N cruise leg 1 in 2015. expo code 33RO20150419. https://doi.org/10.7942/C2WC7C

Wanninkhof, R. (2019b). TCO2 data from P16N cruise leg 2 in 2015. expo code 33RO20150525. https://doi.org/10.7942/C2RP43

Williams, P. M., & Druffel, E. R. M. (1987). Radiocarbon in dissolved organic carbon in the central North Pacific Ocean. *Nature*, *330*(6145), 246–248. https://doi.org/10.1038/330246a0

Xu, X., Trumbore, S. E., Zheng, S., Southon, J. R., McDuffee, K. E., Luttgen, M., & Liu, J. C. (2007). Modifying a sealed tube zinc reduction method for preparation of AMS graphite targets: Reducing background and attaining high precision. *Nuclear Instruments and Methods in Physics Research B*, *259*(1), 320–329. https://doi.org/10.1016/j.nimb.2007.01.175